## Original Article
# Inflammation suppression prevents tumor cell proliferation in a mouse model of thyroid cancer

Sunmi Park[1], Minjun Kim[1], Jack Zhu[2], Woo Kyung Lee[1], Grégoire Altan-Bonnet[3], Paul Meltzer[2], Sheue-Yann Cheng[1]

[1]Laboratory of Molecular Biology, [2]Laboratory of Cancer Biology and Genetics, [3]Cancer and Inflammation Program, Center for Cancer Research, National Cancer Institute, National Institutes of Health, Bethesda, MD 20892, Maryland, USA

**Abstract:** The incidence of thyroid cancer, the most frequent endocrine neoplasia, is rapidly increasing. Significant progress has recently been made in the identification of genetic lesions in thyroid cancer; however, whether inflammation contributes to thyroid cancer progression remains unknown. Using a mouse model of aggressive follicular thyroid cancer (FTC; $Thrb^{PV/PV}Pten^{+/-}$ mice), we aimed to elucidate a cause-effect relationship at the molecular level. The $Thrb^{PV/PV}Pten^{+/-}$ mouse expresses a dominantly negative thyroid hormone receptor β (denoted as PV) and a deletion of a single allele of the $Pten$ gene. These two oncogenic signaling pathways synergistically activate PI3K-AKT signaling to drive cancer progression as in human FTC. At the age of 5-7 weeks, thyroids of $Thrb^{PV/PV}Pten^{+/-}$ mice exhibited extensive hyperplasia accompanied by 77.5-fold infiltration of inflammatory monocytes as compared with normal thyroids. Global gene expression profiling identified altered expression of 2387 genes, among which 1353 were upregulated and 1034 were down-regulated. Further analysis identified markedly elevated expression of inflammation mediators and cytokines such as, $Csf1r$, $Csf1$, $SPP1$, $Aif1$, $IL6$, $Ccl9$, $Ccl3$, $Ccl12$, and $Ccr2$ genes and decreased expression of $Kit$, $Ephx2$, $Cd163$, $IL15$, $Ccl11$, and $Cxcl13$ genes. These changes elicited the inflammatory responses in the hyperplastic thyroid of $Thrb^{PV/PV}Pten^{+/-}$ mice, reflecting early events in thyroid carcinogenesis. We next tested whether attenuating the inflammatory responses could mitigate thyroid cancer progression. We treated the mice with an inhibitor of colony-stimulating factor 1 receptor (CSF1R), pexidartinib (PLX-3397; PLX). CSF1R mediates the activity of the cytokine, colony stimulating factor 1 (CSF1), in the production, differentiation, and functions of monocytes and macrophages. Treatment with PLX decreased 94% and 62% of inflammatory monocytes in the thyroid and bone marrow, respectively, versus controls. Further, PLX suppressed the expression of critical cytokine and inflammation-regulating genes such as $Csf1r$, $SPP1$ $(OPN)$, $Aif1$, $IL6$, $Ccl9$, $Ccl3$, $Ccl12$, and $Ccr2$ (25%-80%), resulting in inhibition of 89% tumor cell proliferation, evidenced by Ki-67 immunostaining. These preclinical findings suggest that inflammation occurs in the early stage of thyroid carcinogenesis and plays a critical in cancer progression. Importantly, attenuation of inflammation by inhibitors such as PLX would be beneficial in preventing thyroid cancer.

**Keywords:** Inflammation, monocytes, colony-stimulating factor 1 receptor, CSF1R inhibitors thyroid cancer, mouse model, pexidartinib (PLX-3397)

## Introduction

The incidence of thyroid cancer, the most frequent endocrine neoplasia, is rapidly increasing. The majority of thyroid cancer arises from thyroid follicular cells. There are three major types of thyroid cancer: differentiated thyroid cancer (DTC) including the papillary and follicular types and anaplastic thyroid cancer (ATC). The prognosis for DTC is favorable, with long-term survival rates of 88% to 93% [1]. However,

ATC has a worse prognosis, with patients rarely surviving beyond 1 year from the time of diagnosis. Recent scientific advances have uncovered molecular pathways responsible for thyroid cancer, leading to the development of specific therapeutics tailored to these molecular changes [2-4]. For thyroid cancer treatment drugs, the most well-known are multiple kinase inhibitors (MKI), targeting the mitogen-activated protein kinase pathway. Although these drugs have shown clinical benefits, the pres-

ence of a tumor-specific resistance mechanism to MKI and the toxicity of the drugs limit clinical benefits [5, 6]. Therefore, a novel treatment strategy is needed for thyroid cancer. One possible strategy is to find regulatory factors that play a major role in the inflammatory tumor microenvironment.

The role of inflammation in DTC has been actively studied in the past decades. Compelling evidence indicates a positive association between chronic inflammation and increased risk of developing DTC. Such a positive link suggested that the inflammatory microenvironment could be an essential component of cellular transformation and tumor progression [7-11]. It was reported that thyroid carcinogenesis is positively affected by inflammatory immune cells and immune-related mediators (e.g., cytokines, interleukins) in addition to the oncogenic changes in the thyroid lesions. Inflammatory cells and mediators enrich the tumor stroma, engaging in tissue remodeling, tissue repair, and neo-angiogenesis [12]. The cancer stroma, also referred to as the tumor microenvironment (TME), clearly has profound influence on thyroid cancer progression. However, it is not clear at what stage of thyroid carcinogenesis inflammation could exert its effects on cancer progression.

In the present studies, we investigated the stage of thyroid carcinogenesis at which inflammation first occurred and how its occurrence could impact thyroid cancer development and progression. We used a mouse model of follicular thyroid cancer (FTC), the $Thrb^{PV/PV}Pten^{+/-}$ mouse. The $Thrb^{PV/PV}Pten^{+/-}$ mouse expresses a potent dominantly negative thyroid hormone receptor β (TRβPV) with a deletion of one allele of the $Pten$ gene. This $Thrb^{PV/PV}Pten^{+/-}$ mouse has previously been shown to fully recapitulate human FTC [13] and has been used as a preclinical model for testing potential molecular targets [14, 15]. In this $Thrb^{PV/PV}Pten^{+/-}$ mouse, the cancer progression is driven by over-activation of PI3K-AKT signaling due to the oncogenic actions of TRβPV and PTEN-deficiency [13].

We evaluated the inflammatory responses at the age of ~1.5 months, when the thyroid follicular cells were actively proliferating (hyperplasia) driven by PI3K-AKT signaling. We found that extensive hyperplasia was accompanied by active infiltration of inflammatory mono-

cytes, macrophages, and their mediators such as immune-related regulators, interleukins, and cytokines. Importantly, the inflammatory responses were attenuated by an inhibitor of colony-stimulating factor 1 receptor (CSF1R), pexidartinib (PLX-3397; PLX), concurrently with the inhibition of hyperplasia of thyroid follicular cells. Our studies showed that inflammatory responses were initiated as early as the beginning stage of hyperplasia during thyroid carcinogenesis. These results suggest that attenuation of inflammation at the early stage of carcinogenesis could prevent cancer development.

## Materials and methods

### Mice and treatment

Generation of $Thrb^{PV/PV}Pten^{+/-}$ mice was described in previous studies [13]. Treatment of PLX3397 (Pexidartinib; BOC Sciences Shirley, NY) was started from 6- to 7-weeks old. Mice were given PLX3397 doses of 50 mg/kg via oral gavage daily for 10 days. PLX3397 was dissolved in 10% DMSO and corn oil (sigma-Aldrich, St. Louis, MO). The animal study was performed according to the approved protocols of the National Cancer Institute Animal Care and Use Committee.

### Flow cytometry analysis

The sources of antibodies and fluorophore-labeled antibodies used in FACS analyses are listed in Table S1. Blood samples were collected and their red blood cells were lysed using an ACK lysis buffer (Quality Biological, Gaithersburg MD). Single cells from thyroid tissue were prepared by physical dissociation. First, cell suspensions were incubated with Fc receptor blocking Abs (CD16/CD32, Thermo Fisher Scientific, Waltham, MA) for 15 minutes on ice and incubated for 30 minutes with indicated mouse antibodies on ice and washed with PBS + 2% BSA buffer. The antibodies used were listed in (Table S1). Stained cells were analyzed using a BD Fortessa II flow cytometer (BD Biosciences, San Jose, CA). FACS measurements were compensated and analyzed using FlowJo, LLC (Tree Star Inc, Ashland, OR).

### Immunohistochemistry

The thyroid tumor was removed from $Thrb^{PV/PV}Pten^{+/-}$ mice and PLX3397-treated $Thrb^{PV/}$

$^{PV}Pten^{+/-}$ mice. The isolated thyroid tumor was flushed with ice-cold 1 × phosphate-buffered saline (PBS) and fixed in 4% formaldehyde (and, if needed, stored at 4°C), followed by embedding in paraffin and then cutting into 5-μm sections. Immunohistochemistry (IHC) was performed by the standard method. Primary antibodies for OPN antibody (1:200 dilution) and NF-κB p65 (1:500 dilution) were purchased from Abcam (Cambridge, MA). F4/80 (1:200 dilution) antibody was purchased from Thermo Fisher Scientific (Waltham, MA) for IHC. A primary antibody was incubated at 4°C for 24 hours. The secondary antibody was developed with diaminobenzidine (DAB). The sections were counterstained with hematoxylin. Results were reviewed and verified by two observers.

*RNA extraction and RT-qPCR*

Total RNA was isolated from thyroid tissues using Pure Link™ RNA mini kit (Thermo Fisher Scientific, Waltham, MA). RT-qPCR was performed with One-Step SYBR Green RT-qPCR Master Mix (Qiangen, Valencia, CA). The mRNA level of each gene was normalized by GAPDH (glyceraldehyde-3-phosphatedehydrogenase). The primer sequences are listed in Table S2.

*RNA quality analysis and microarray*

Total RNA from thyroid tissues was isolated using Trizol (Thermo Fisher Scientific, Waltham, MA). Quality of RNA was confirmed with the Agilent RNA 6000 Nano Kit (Agilent Technologies, Santa Clara, CA). Total RNA was used for the expression analysis using Affymetrix Clariom S arrays (Thermo-Fisher, Grand Island, NY) according to the manufacturer's protocol. Transcriptome Analysis Console (TAC) version 4.0 (Applied Biosystems) was used for data processing and analysis. Differential expressed genes were selected by the following criteria: Fold change ≥2 and adj. *p*-value ≤0.05.

*Statistical analysis*

All statistical analyses and the graphs were performed and generated using GraphPad Prism version 7.0 (GraphPad Software, La Jolla, CA). $P < 0.05$ is considered statistically significant. All data are expressed as mean ± SEM.

## Results

*Increased filtration of inflammatory monocytes in hyperplastic stage of thyroid carcinogenesis*

We have previously shown that thyroid carcinogenesis in the $Thrb^{PV/PV}Pten^{+/-}$ mouse progresses through the stages of hyperplasia, capsular invasion, vascular invasion, anaplasia, to eventual metastasis [13]. This pathological progression is similar to human FTC. We recently reported a large influx of inflammatory monocytes into the thyroid tumors of $Thrb^{PV/PV}Pten^{+/-}$ mice aged 5-7 months, at which time cancer is at the advanced stage (mice were moribund) [16]. To ascertain whether such infiltration occurs at the early stage of thyroid carcinogenesis, we analyzed inflammatory monocytes in the thyroid, bone marrow, and blood of $Thrb^{PV/PV}Pten^{+/-}$ mice at the age of 5-7 weeks. At this beginning stage of thyroid carcinogenesis, thyroid follicular cells were actively proliferating in response to the activated PI3K-AKT signaling driven by oncogenic TRβPV mutant and the haplodeficiency of the *Pten* gene in $Thrb^{PV/PV}Pten^{+/-}$ mice [13]. Using a series of surface markers, we analyzed inflammatory monocytes in the thyroid, bone marrow and blood (**Figure 1A1-C1**, respectively). Our gating strategy in the flow cytometry analysis (FACS) was first to gate out leukocyte population [CD115$^+$Lineage$^-$ (CD3-CD19-NKp46-Ter1 19-Ly6G-Scal$^-$], followed by selection of matured monocytes using CD11b$^+$cKit$^-$ population. Analysis of FACS data showed that the percentage of inflammatory monocyte population in the Ly6C$^+$ClassII$^+$ area in thyroid of $Thrb^{PV/PV}Pten^{+/-}$ mice was 77.5-fold that in normal thyroid of wild-type mice (**Figure 1A2**). However, no significant changes in the inflammatory monocytes were detected in the bone marrow, nor in the blood between $Thrb^{PV/PV}Pten^{+/-}$ and WT mice (**Figure 1B1** and **1C2**, respectively). These results indicated that inflammatory monocytes were accumulated in the thyroid of $Thrb^{PV/PV}Pten^{+/-}$ mice when thyrocytes were undergoing active proliferation at the early phase of thyroid carcinogenesis.

*Alterations in the global gene expression profiles in thyroid follicular cells of $Thrb^{PV/PV}Pten^{+/-}$ mice*

To delineate the molecular mechanism leading to increased inflammatory monocytes in $Thrb^{PV/PV}Pten^{+/-}$ mice at the age of 5-7 weeks, we
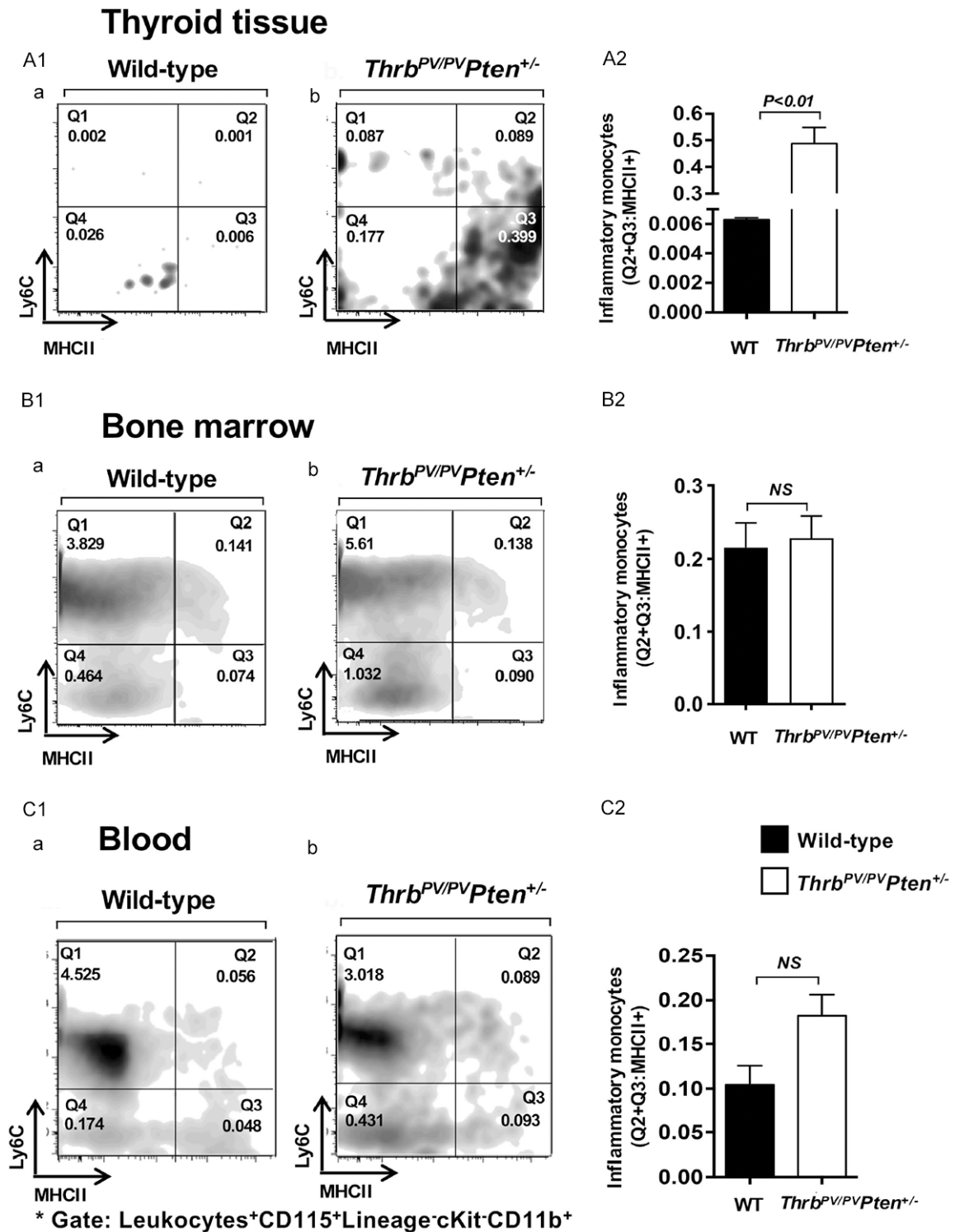
**Figure 1.** Increased inflammatory monocytes in the thyroid of *Thrb$^{PV/PV}$Pten$^{+/-}$* Mice. (A1-C1) Analysis of monocyte population in the thyroid tissue (A1), bone marrow (B1), and blood (C1) of wild-type (a) and *Thrb$^{PV/PV}$Pten$^{+/-}$* mice (b) by FACS analysis. Classification of monocytes in the thyroid tissue (A1), bone marrow (B1), and blood (C1) was analyzed by using Ly6C and MHCII antibodies after gating in leukocytes + CD115 + Lineage (CD3-CD19-NKp46-Ter119-Ly6G-Sca1$^-$)cKit$^-$ CD11b$^+$ population. (A2-C2) Inflammatory monocytes were defined cells in MHCII+ population (Q2 and Q3 in A1, B1, and C1). Shown is the quantification of percentage of inflammatory monocytes in the thyroid tissue (A2), bone marrow (B2), and blood (C2) of wild-type (n = 5-8) and *Thrb$^{PV/PV}$Pten$^{+/-}$* mice (n = 6). Values are means ± SEM. The *p* values are indicated. NS, not significant.
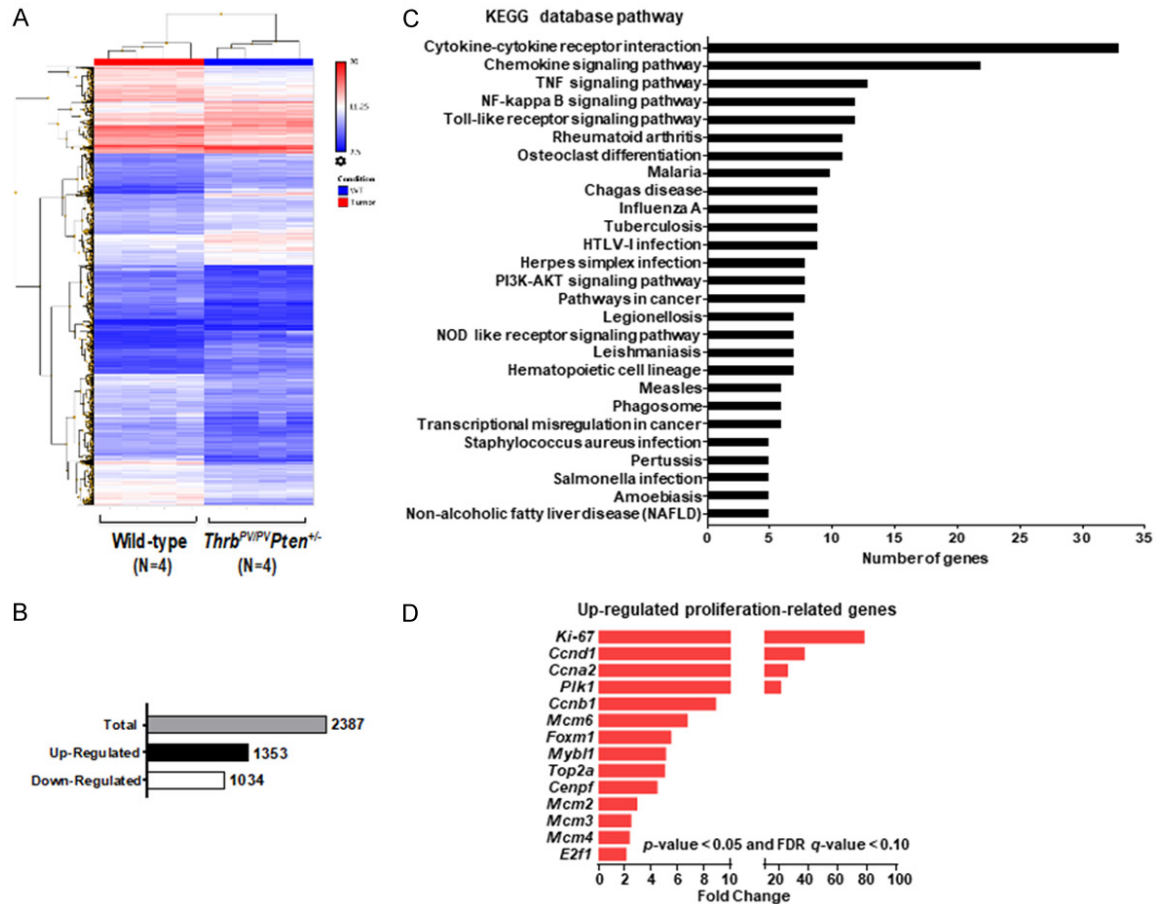
**Figure 2.** Comparison of gene expression profiles of wild-type and $Thrb^{PV/PV}Pten^{+/-}$ mice. A. Heat map showed the differential expression in thyroid tissues of wild-type (n = 4) and $Thrb^{PV/PV}Pten^{+/-}$ mice (n = 4). B. Of 2,387 genes differentially altered in thyroid tumors of $Thrb^{PV/PV}Pten^{+/-}$ mice versus wild-type mice, 1,353 were up-regulated and 1,034 were down-regulated. C. Shown are the most consistent hallmark pathways of immune-related target genes in thyroid of $thrb^{PV/PV}Pten^{+/-}$ mice ($P$ < 0.05 and fold change > 2). D. Proliferation-related genes enriched in the hyperplastic follicular cells of $Thrb^{PV/PV}Pten^{+/-}$ mice (n = 4) compared to wild-type mice (n = 4). Genes with $p$-value < 0.05 and FDR $q$-value < 0.10 were considered as statistically significant.

acquired the transcriptional profile of $Thrb^{PV/PV}Pten^{+/-}$ thyroid tumors from $Thrb^{PV/PV}Pten^{+/-}$ mice and wild-type (WT) mice using microarray analysis. Hierarchical clustering of the differentially expressed genes showed that expression patterns in the thyroids between WT and $Thrb^{PV/PV}Pten^{+/-}$ mice were distinct (**Figure 2A**). We identified 2387 differentially expressed genes, among which 1353 were up-regulated and 1034 were down-regulated (**Figure 2B**). Additional functional enrichment analysis showed 63 inflammation-related genes that were further classified based on KEGG pathway data. Pathway overrepresentation analysis showed highly ranked multiple genes related to cytokine-cytokine receptor interaction, chemokine signaling pathway, and tumor necrosis factor (TNF) signaling pathway (**Figure 2C**). These

results revealed that increased inflammatory monocytes in the thyroid of $Thrb^{PV/PV}Pten^{+/-}$ mice are correlated with inflammatory mediators such as chemokines, cytokines, and interleukins.

At the age of 5-7 weeks, thyroid follicular cells of $Thrb^{PV/PV}Pten^{+/-}$ mice exhibited extensive hyperplasia. To ascertain what genes were involved in the hyperplasia of follicular cells at the beginning of thyroid carcinogenesis, we further analyzed the gene expression in up-regulated gene group (**Figure 2B**). We identified a large group proliferation-related genes which are the key players in each phase of cell cycle progression, such as $Ki$-$67$ (all phases of cell cycle progression), $Ccnd1/E2f1$ (G1-S), $Ccna2$ (S-G2), $Plk1/Ccnb1$ (G2-M), and $Mcm$ families

**Table 1.** Up-regulated immune-related genes in the thyroid of $Thrb^{PV/PV}Pten^{+/-}$ mice

|  | Gene | Gene name | Fold change |
|---|---|---|---|
| Inflammation-regulators | Csf1 | colony stimulating factor 1 | 20.33 |
|  | Csf1r | colony stimulating factor 1 receptor | 6.88 |
|  | Spp1 | secreted phosphoprotein 1 | 414.05 |
|  | Ptgs1 | prostaglandin-endoperoxide synthase 1 | 37.73 |
|  | Aif1 | allograft inflammatory factor 1 | 13.74 |
|  | Sphk1 | sphingosine kinase 1 | 5.25 |
|  | Chil1 | chitinase-like 1 | 5.82 |
| Interleukins | Il1f6 | interleukin 1 family, member 6 | 7.14 |
|  | Il24 | interleukin 24 | 4.74 |
|  | Il6 | interleukin 6 | 3.74 |
|  | Il1a | interleukin 1 alpha | 2.26 |
| Cytokines | Ccl9 | chemokine (C-C motif) ligand 9 | 25.1 |
|  | Ccl3 | chemokine (C-C motif) ligand 3 | 14.81 |
|  | Ccl12 | chemokine (C-C motif) ligand 12 | 13.31 |
|  | Ccl8 | chemokine (C-C motif) ligand 8 | 6.07 |
|  | Ccl6 | chemokine (C-C motif) ligand 6 | 5.09 |
|  | Ccl20 | chemokine (C-C motif) ligand 20 | 3.58 |
|  | Ccl2 | chemokine (C-C motif) ligand 2 | 2.84 |
|  | Ccl5 | chemokine (C-C motif) ligand 5 | 2.67 |
|  | Ccr2 | chemokine (C-C motif) receptor 2 | 4.37 |
|  | Ccr1 | chemokine (C-C motif) receptor 1 | 2.51 |
|  | Cxcl11 | chemokine (C-X-C motif) ligand 11 | 9.22 |
|  | Cxcl2 | chemokine (C-X-C motif) ligand 2 | 2.32 |

(late M-G1) (**Figure 2D**). Of note, the expression of *Ki-67, Ccnd1, Ccna2,* and *Plk1* gene was more than 20-fold higher in the hyperplastic follicular cells of $Thrb^{PV/PV}Pten^{+/-}$ mice, compared to wild-type, indicating aberrant cell-cycle progression.

We next selected top-ranking genes for further characterization. **Table 1** shows the up-regulated immune-related genes in thyroid of $Thrb^{PV/PV}Pten^{+/-}$ mice compared to WT. The fold-changes values ranged from 2.32-fold up to 414.05-fold. These up-regulated genes can be sub-categorized into three major classes: inflammation-regulators, interleukins, and cytokines (**Table 1**). The expression of inflammation-regulator genes such as *Csf1, Csf1r, Spp1 (OPN), Ptgs1, Aif1, Sphk1,* and *Chil1* was elevated 5.25- to 414.05-fold in the thyroid of $Thrb^{PV/PV}Pten^{+/-}$ mice. The expression of interleukin genes such as *Il1f6, Il1a, Il6,* and *Il24* was also increased (2.26- to 7.14-fold); there was also increased expression of the cytokine genes *Ccl2, Ccl3, Ccl5, Ccl6, Ccl8, Ccl9, Ccl12, Ccl20, Ccr1, Ccr2, Cxcl11,* and *Cxcl12* (2.32- to

25.1-fold). The expression of many up-regulated genes was further validated by RT-PCR. Consistent with RNA-seq data, mRNA expression of those critical genes was increased in the thyroid of $Thrb^{PV/PV}Pten^{+/-}$ mice: *Csf1* (7.5-fold), *Csf1r* (6.5-fold), *Spp1* (OPN, 70.5-fold), *Aif1* (8.5-fold), *Il6* (11.5-fold), *Ccl9* (10.5-fold), *Ccl3* (23.5-fold), *Ccl12* (13.4-fold), and *Ccr2* (6.5-fold) (**Figure 3A**, panels a-i). **Table 2** shows the down-regulated immune-related genes in the thyroid of $Thrb^{PV/PV}Pten^{+/-}$ mice as compared with WT. The fold changes ranged from 2.1- to 79.65-fold. We also sub-classified these down-regulated genes into three different groups as shown in **Table 2**: inflammation-regulator genes (*Kit, Ephx2,* and *CD163,* ranging from 2.78- to 7.89-fold), interleukin genes (*Il15* and *Il17r,* ranging from 3.31- to 3.94-fold), and cytokines (*Cxcl13, Ccl11, Ccl21b,* and *Ccl1c,* ranging from 2.1- to 79.65-fold).

We further validated the down-regulation of these genes by qRT-PCR. Consistent with RNA-seq data, mRNA expression of those critical genes was decreased in the thyroid of *Thrb^{PV/*
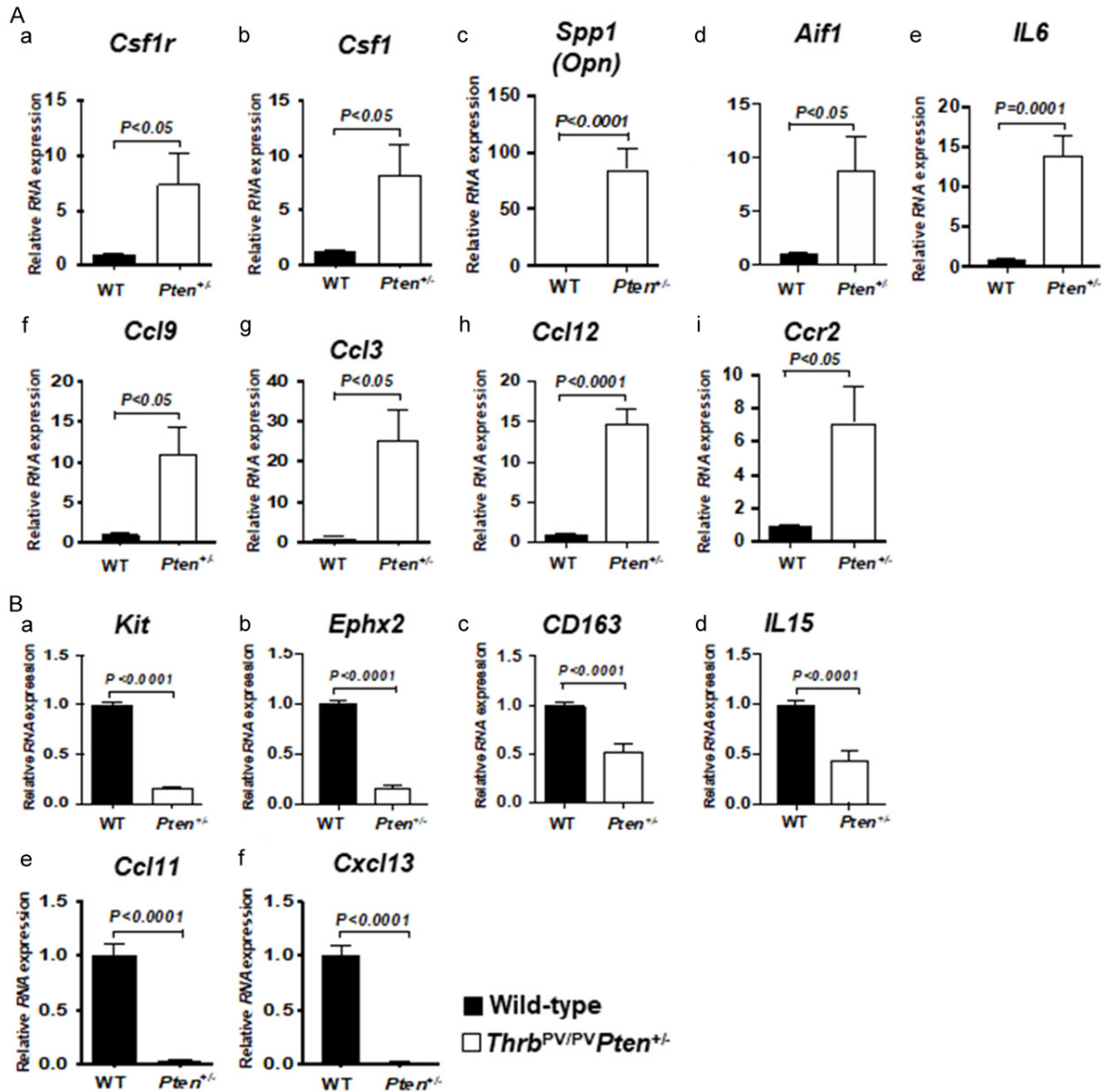
**Figure 3.** Alteration of inflammation-related genes in the thyroid of $Thrb^{PV/PV}Pten^{+/-}$ mice (A). qPCR results for up-regulated inflammation modulators for *Csf1r* (a), *Ctsf1* (b), *Spp1 (OPN)* (c), *Aif1* (d), *IL6* (e), *Ccl9* (f), *Ccl3* (g), *Ccl12* (h), and *Ccr2* (i) in the thyroid of $Thrb^{PV/PV}Pten^{+/-}$ mice (n = 4) compared with wild-type mice (n = 4). The mRNA level of each gene was normalized to the *GAPDH (glyceraldehyde-3-phosphate dehydrogenase)* mRNA level. Values are means ± SEM. The *p* values are indicated. (B) qPCR results for down-regulated inflammation modulators for *Kit* (a), *Ephx2* (b), *CD163* (c), *IL15* (d), *Ccl11* (e), and *Cxcl13* (f) in the thyroid of $thrb^{PV/PV}Pten^{+/-}$ mice (n = 4) compared with wild-type mice (n = 4). The mRNA level of each gene was normalized to the *GAPDH* mRNA level. Values are means ± SEM. The *p* values are indicated.

$^{PV}Pten^{+/-}$ mice: *Kit* (8.1-fold), *EPhx2* (5-fold), *CD163* (2-fold), *IL15* (2.3-fold), *Ccl11* (13.5-fold), and *Cxcl13* (16.5-fold) (**Figure 3B**, panels a-f). Taken together, the changes in these immune-related genes elicited the inflammatory responses in the thyroid of $Thrb^{PV/PV}Pten^{+/-}$ mice, reflecting early events in thyroid carcinogenesis.

*Suppression of inflammatory responses inhibits hyperplasia in the thyroid of $Thrb^{PV/PV}Pten^{+/-}$ mice*

To demonstrate the functional relevance of inflammatory responses in thyroid carcinogenesis, we tested the hypothesis that suppression of inflammation could impede thyroid can-

**Table 2.** Down-regulated immune-related genes in the thyroid of *Thrb^{PV/PV}Pten^{+/-}* mice

| | Gene | Gene name | Fold change |
|---|---|---|---|
| Inflammation-regulators | Kit | kit oncogene | -7.89 |
| | Ephx2 | epoxide hydrolase 2, cytoplasmic | -3.64 |
| | Cd163 | CD163 antigen | -2.78 |
| Interleukins | Il15 | interleukin 15 receptor, alpha chain | -3.94 |
| | Il17re | interleukin 17 receptor E | -3.31 |
| Cytokines | Cxcl13 | chemokine (C-X-C motif) ligand 13 | -79.65 |
| | Ccl11 | chemokine (C-C motif) ligand 11 | -33.92 |
| | Ccl21b | chemokine (C-C motif) ligand 21B | -2.1 |
| | Ccl21c | chemokine (C-C motif) ligand 21C | -2.3 |

cer progression in *Thrb^{PV/PV}Pten^{+/-}* mice. Among the genes with increased expression in the thyroid of *Thrb^{PV/PV}Pten^{+/-}* mice (see **Table 1**), one critical inflammation regulator, colony-stimulating factor 1 receptor [CSF1R; also known as macrophage colony-stimulating factor receptor (M-CSFR; or CD115/cluster of differentiation 115)], caught our attention (**Table 1** and **Figure 3Ab**). It acts as a receptor for colony stimulating factor 1 (CSF1), which controls the production, differentiation, and function of macrophages [17, 18]. The expression of the *Csf1r* gene was up-regulated 6.5-fold in the thyroid of *Thrb^{PV/PV}Pten^{+/-}* mice (**Figure 3Aa**). Moreover, the expression of the *Csf1* gene (the cytokine) was also elevated 7.5-fold in the thyroid of *Thrb^{PV/PV}Pten^{+/-}* mice (**Figure 3Ab**). We therefore chose to target CSF1R by using an inhibitor, pexidartinib (PLX-3397; PLX). PLX is a novel tyrosine kinase inhibitor that targets CSF1R to reduce tissue macrophage levels [19]. We treated *Thrb^{PV/PV}Pten^{+/-}* mice with PLX and evaluated its efficacy by comparing inflammatory monocytes in the thyroid, bone marrow, and the blood. Compared with the vehicle-treated *Thrb^{PV/PV}Pten^{+/-}* mice, PLX treatment decreased percentage of inflammatory monocyte population in the thyroid as shown by FACS (Q2+Q3 areas) (**Figure 4A1**, compare panel b with panel a). The monocytes were also lowered in the bone marrow (**Figure 4B1**, compare panel b with panel a). However, we found no apparent differences in the number of monocytes in the blood between the PLX-treated or vehicle-treated *Thrb^{PV/PV}Pten^{+/-}* mice (**Figure 4C1**, compare panel b with panel a). The results can be seen more clearly by the quantitative analyses shown in **Figure 4A2** and **4B2** in that monocytes were 93.8% and 61.9% lower in the thyroid and bone marrow, respectively, of PLX-treated mice than in vehicle-treated mice. In **Figure 4C2**, no significant differences of monocytes were observed in the blood of PLX-treated and vehicle-treated *Thrb^{PV/PV}Pten^{+/-}* mice. These data indicated that PLX was effective in reducing the number of inflammatory monocytes in the thyroid and bone marrow.

We next ascertained whether the macrophages were also decreased in the thyroid of PLX-treated *Thrb^{PV/PV}Pten^{+/-}* mice by immunochemical analysis using the anti-F4/80 antigen, which is a mature mouse cell surface glycoprotein expressed at high levels on macrophages. We found that F4/80-positive signals were reduced in the thyroid of PLX-treat *Thrb^{PV/PV}Pten^{+/-}* mice (compare panel d with panel c, **Figure 4D1**). Panels a and b of **Figure 4D1** are the IgG controls. Quantitative analysis showed a 60% reduction of F4/80-positive cells in the thyroid of PLX-treated *Thrb^{PV/PV}Pten^{+/-}* mice (**Figure 4D2**). These data indicated that macrophages in the thyroid were effectively lowered by PLX treatment.

*PLX-3397 treatment altered the expression of inflammatory regulators and cytokines in the thyroid of Thrb^{PV/PV}Pten^{+/-} mice*

We have shown that increased infiltration of inflammatory monocytes in the thyroid of *Thrb^{PV/PV}Pten^{+/-}* mice led to up-regulation of a panel of inflammatory regulators and cytokines (see **Figure 3A** and **Table 1**). With the reduced infiltration of inflammatory monocytes in the thyroid by PLX treatment (**Figure 4A1**), we investigated whether the expression of these up-regulated inflammatory regulators and cytokines would be affected by PLX treatment. Indeed, we found that PLX inhibited the expres-

A1 **Thyroid**
a vehicle
b PLX-3397

A2

B1 **Bone marrow**
a vehicle
b PLX-3397

B2

C1 **Blood**
a vehicle
b PLX-3397

C2

* Gate: Leukocytes⁺CD115⁺Lineage⁻cKit⁻CD11b⁺

D1
Vehicle    PLX-3397
IgG Control
Anti-F4/80

D2
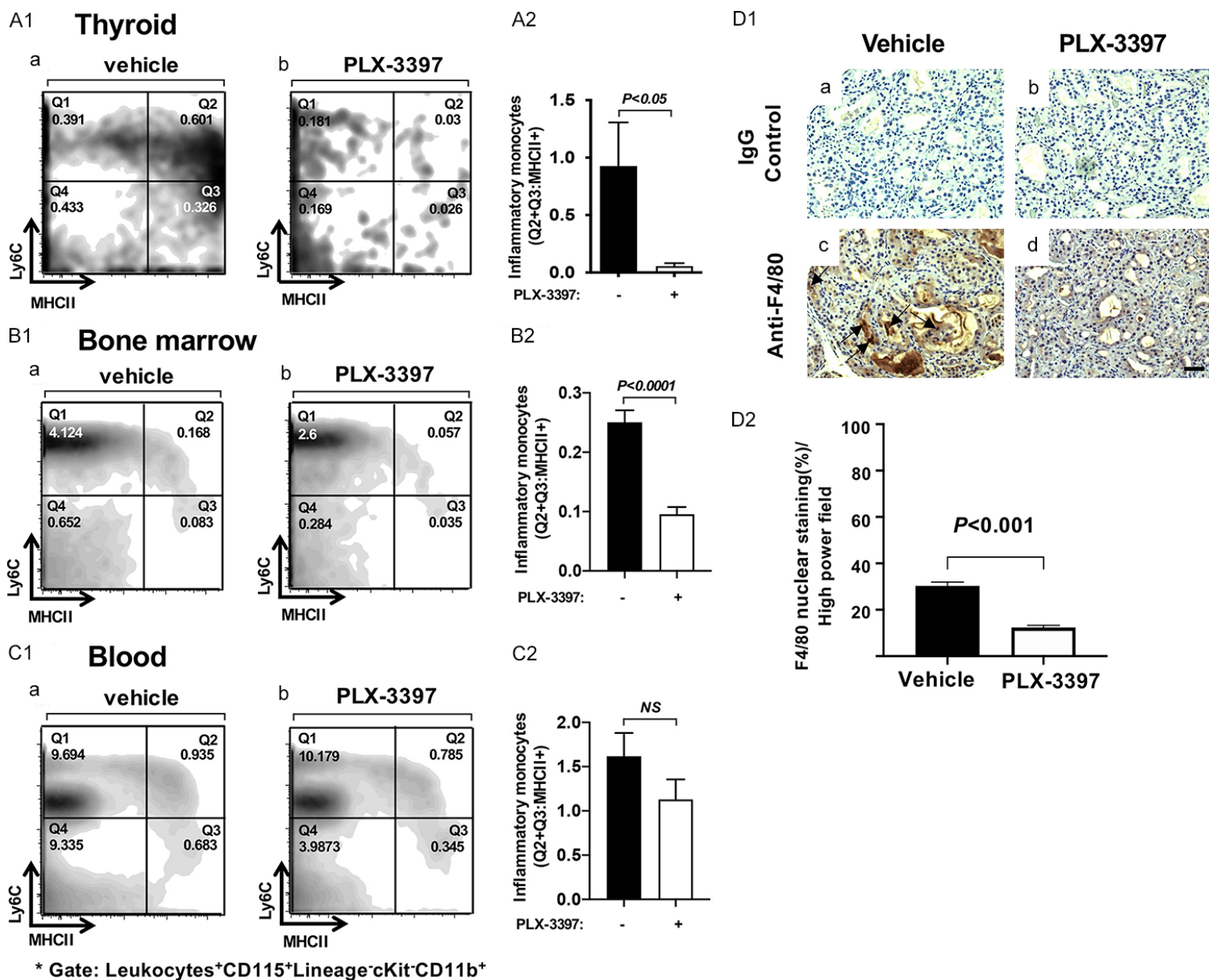
**Figure 4.** Decrease in inflammatory monocytes in the thyroid and bone marrow of *hrb^{PV/PV}Pten^{+/-}* mice after PLX treatment. PLX was administered daily via oral gavage at a dose of 50 mg/kg for 10 days in *Thrb^{PV/PV}Pten^{+/-}* mice. Analysis of monocyte population in the thyroid tissue (A1), bone marrow (B1), and blood (C1) of *Thrb^{PV/PV}Pten^{+/-}* mice treated with vehicle (a) and PLX treatment (b) by FACS analysis. Classification of monocytes in the thyroid tissue (A1), bone marrow (B1), and blood (C1) was performed by using Ly6C and MHCII antibodies after gating in leukocytes + CD115 + Lineage (CD3-CD19-NKp46-Ter119-Ly6G-Sca1-)⁻cKit⁻ CD11b⁺ population. (A2-C2) Inflammatory monocytes were defined cells in MHCII⁺ population (Q2 and Q3 in A1-C1). Quantification of % inflammatory monocytes in the thyroid tissue (A2), bone marrow (B2), and blood (C2) of *Thrb^{PV/PV}Pten^{+/-}* mice treated with vehicle (n = 3) and PLX-3397 treatment (n = 3). Values are means ± SEM. The *p* values are indicated. (D1) Representative immunohistochemically stained micrographs with an antibody against F4/80 antigen in formalin-fixed thyroid slides of *Thrb^{PV/PV}Pten^{+/-}* mice treated with vehicle (n = 3) (c) or PLX (n = 3) (d). The positively stained cells are marked by arrows (c). The negative control panels using IgG are shown in the corresponding panels (a and b). (D2) Graphs indicate the quantification for percentage of F4/80 positively staining cells in the thyroid of *Thrb^{PV/PV}Pten^{+/-}* mice treated with vehicle or PLX. Values are means ± SEM. The *p* values are indicated. NS, not significant.

sion of *Csf1r* by 50.7% in the thyroid of PLX-treated *Thrb^{PV/PV}Pten^{+/-}* mice (panel a, **Figure 5A**). Intriguingly, the expression of *Csf1* was elevated by 2.2-fold in the thyroid of PLX-treatment (**Figure 5A**, panel b). However, the expression of other major inflammatory regulators, interleukins, and cytokines such as *Spp1*, *Aif1*, *Il6*, *Ccl9*, *Ccl3*, *Ccl12*, and *Ccr2* was reduced by PLX, ranging from 24% to 80% reduction as compared with controls (**Figure 5A**, panels c-i). The increased infiltration of inflammatory monocytes in the thyroid of *Thrb^{PV/PV}Pten^{+/-}* mice also led to down-regulation of a panel of inflammatory regulators and cytokines (shown in **Figure 3B** and **Table 2**). We ascertained whether the expression of these genes would be affected by PLX treatment. The expressions of *kit, ephx2, IL15,* and *Cxcl13* were elevated by 42% to 132% after treatment with PLX (**Figure 5B**, panels a, b, d, and f), whereas the expressions of *CD163* and *Ccl11* were reduced by PLX treatment (**Figure 5B**, panels c and e). Taken together, the changes in the expression of inflammatory regulators, interleukins, and cytokines reflected the significant impact of PLX treatment on the inflammatory landscape of thyroid in *Thrb^{PV/PV}Pten^{+/-}* mice.

*PLX-3397 treatment inhibits proliferation of thyroid follicular cells of Thrb^{PV/PV}Pten^{+/-} mice*

Among the up-regulated genes associated with the increased infiltration of inflammatory monocytes was the *Sppl* (*Opn*) gene. Its mRNA expression was the most highly expressed among all up-regulated gene with increases by a remarkable 70.5-fold (see **Figure 3A**, panel c). Previously, we showed that OPN interacts with cell surface receptors, such as integrin β1, to activate the down-stream PI3K-AKT and NF-κB signaling to increase cell proliferation

[20, 21]. Thus, the up-regulation of the *Opn* gene during inflammatory responses at the early stage of thyroid carcinogenesis could contribute to hyperplasia of the follicular cells. Importantly, we found the PLX treatment suppressed the mRNA expression of the *Opn* gene in the thyroid (**Figure 5Ac**).

We therefore performed IHC analysis to determine whether the OPN protein levels were also lowered by PLX treatment and found this was indeed the case (**Figure 6A1**, compare panel d with c). Quantitative analysis showed the number of follcular cells with OPN-positive signal was decreased 81.2 % (**Figure 6A2a**). Similarly, we found that PLX treatment lowered the p65 (active form of NFκB) protein levels (**Figure 6A1**, compare panel f with e). Quantitative analysis showed the number of follcular cells with p65-positive signal was decreased by 77.6% (**Figure 6A2b**). To validate that the reduced protein levels of OPN and p65 led to suppressed proliferation of thyroid follicular cells, we analyzed the extent of follicular cell proliferation by using cell proliferation marker, Ki-67. Ki-67 is one of highly up-regulated gene during hyperplasia of follicular cells of thyroid carcinogenesis (see **Figure 2D**). PLX treatment markely lowered the Ki-67 marker protein (**Figure 6B1**, compare panel d with c). Quantitative analysis showed the number of follcular cells with Ki-67-positive signal was greatly decreased by 88.5% (**Figure 6B2**), indicativative of profound inhibition of proliferatioin of thyoid follicule cells. These results clearly show that PLX was effective in suppressing the expression of inflammatory regulators and cytokins. Such suppression led to the inhibition of the down-stream signaling to inhibit folliclar cell proliferation to prevent subsequent thyroid tumor development (see **Figure 7**).
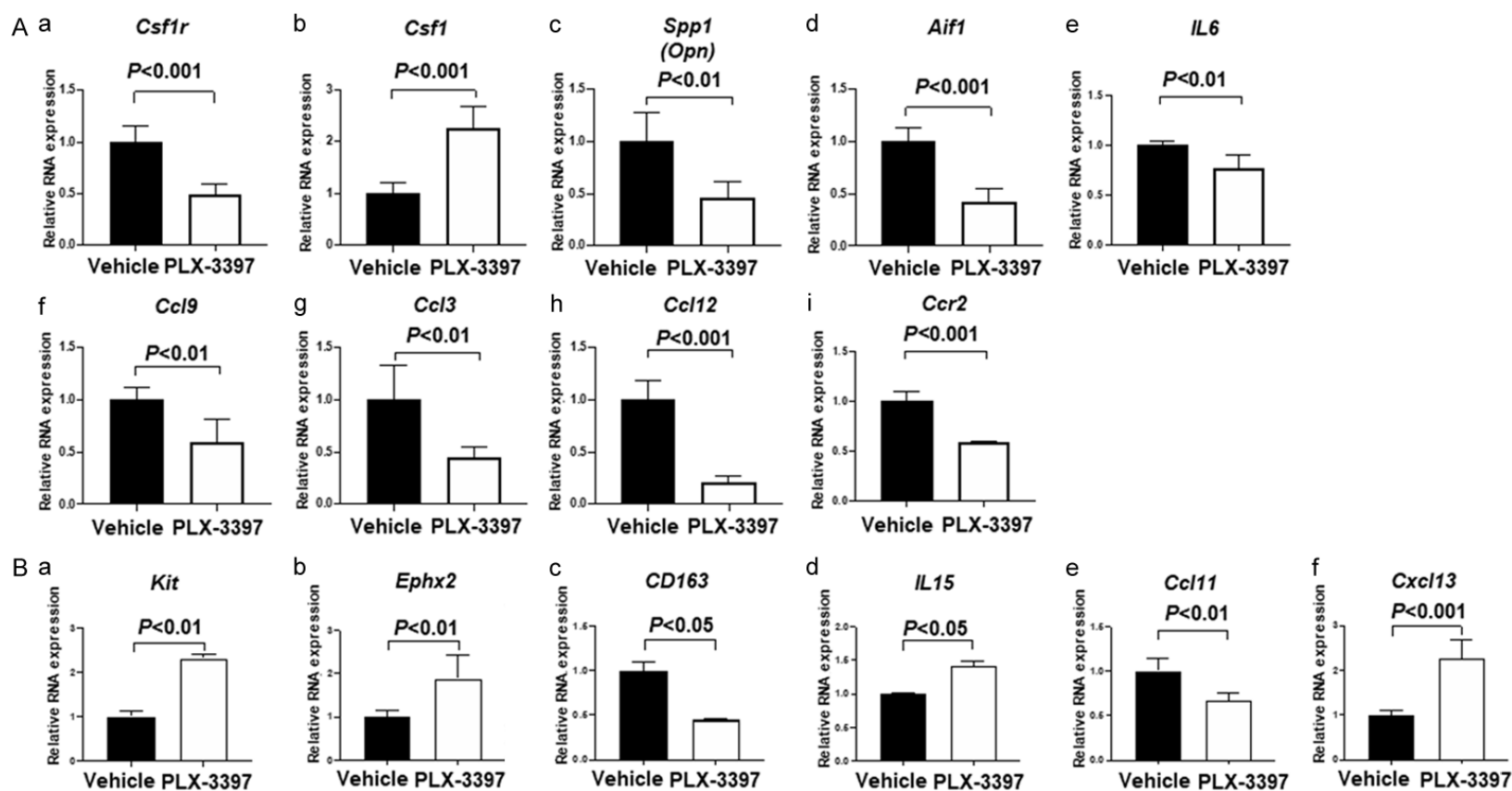
**Figure 5.** Altered expression of inflammatory regulators, cytokines in the thyroid of $Thrb^{PV/PV}Pten^{+/-}$ mice after PLX treatment. A. qPCR results for inflammation modulators *Csf1r* (a), *Ctsf1* (b), *Spp1 (OPN)* (c), *Aif1* (d), *IL6* (e), *Ccl9* (f), *Ccl3* (g), *Ccl12* (h), and *CCR2* (i) in the thyroid of vehicle-treated $Thrb^{PV/PV}Pten^{+/-}$ mice (n = 3) compared with PLX-treated $Thrb^{PV/PV}Pten^{+/-}$ mice (n = 3). The mRNA level of each gene was normalized to the *GAPDH* mRNA level. Values are means ± SEM. The p values are indicated. B. qPCR results for inflammation modulators *Kit* (a), *Ephx2* (b), *CD163* (c), *IL15* (d), *Ccl11* (e), and *Cxcl13* (f) in the thyroid of vehicle-treated $Thrb^{PV/PV}Pten^{+/-}$ mice (n = 3) compared with PLX-3397 treated $Thrb^{PV/PV}Pten^{+/-}$ (n = 3). The mRNA level of each gene was normalized to the *GAPDH* mRNA level. Values are means ± SEM. The p values are indicated.
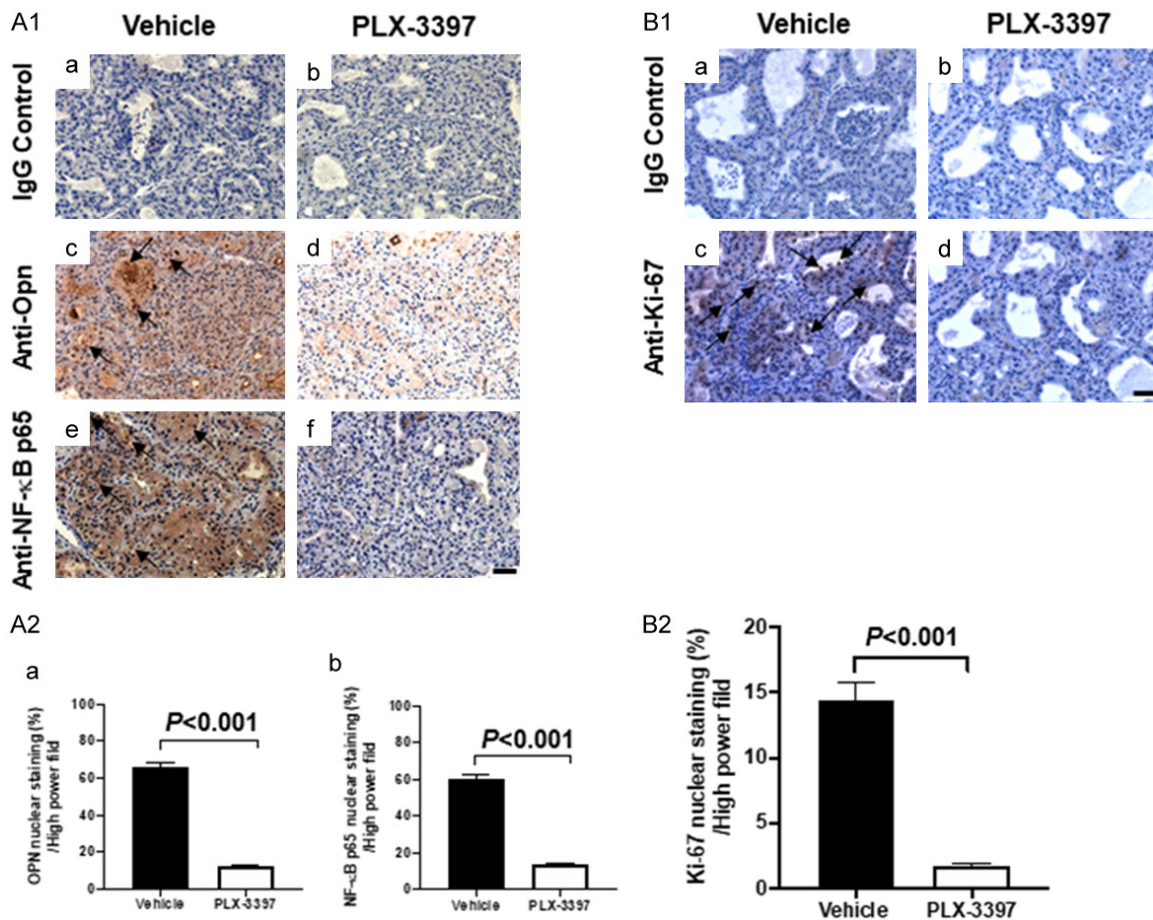
**Figure 6.** Immunohistochemical analysis of proliferation markers in the thyroid of $Thrb^{PV/PV}Pten^{+/-}$ mice. (A1) Representative immunohistochemically stained micrographs with an antibody against OPN (c and d), NF-κB p65 (e and f) in formalin-fixed thyroid slides of $Thrb^{PV/PV}Pten^{+/-}$ mice treated with vehicle (n = 3) and PLX (n = 3). The positively stained cells are marked by arrows (c and e). The negative control panels using IgG are shown in the corresponding panels (a and b). (A2) Graphs indicate quantification of percentage of positively stained cells of OPN (a in A-II), NF-κB p65 and (b in A2) in the $Thrb^{PV/PV}Pten^{+/-}$ mice treated with vehicle (n = 3) or PLX (n = 3). (B1) Representative immunohistochemically stained micrographs with an antibody against Ki-67 (c and d) in formalin-fixed thyroid slides of $Thrb^{PV/PV}Pten^{+/-}$ mice treated with vehicle (n = 3) or PLX (n = 3). (B2) Graphs indicate quantification of percentage of positively stained cells of Ki-67 in the thyroid of $Thrb^{PV/PV}Pten^{+/-}$ mice treated with vehicle (n = 3) or PLX (n = 3). Values are means ± SEM. The $p$ values are indicated.

## Discussion

Recently, interest in understanding how inflammation could impact thyroid carcinogenesis has steadily increased. Despite progress in demonstrating a link between the two, many questions remain. One essential question concerns the stage of cancer development at which inflammation responses occur that could direct the course of thyroid carcinogenesis. Using a mouse model of FTC, we aimed to address this question. We showed that at the young age of 5-7 weeks, while thyroid follicular cells were actively proliferating driven by overactivated PI3K-AKT signaling, there was a con-

current infiltrating of inflammatory monocytes (See **Figure 1**) and macrophages (**Figure 4D1**, panel c). Furthermore, extensive changes in the expression of inflammatory regulators, interleukins, and cytokines were detected to accompany the increases of inflammatory monocytes. The present studies demonstrated for the first time that inflammatory responses occurred concurrent with the hyperplastic stage of thyroid follicular cells in the carcinogenesis process.

Two types of pathways have been proposed to understand how inflammation links to thyroid cancer progression: the extrinsic (microenvi-
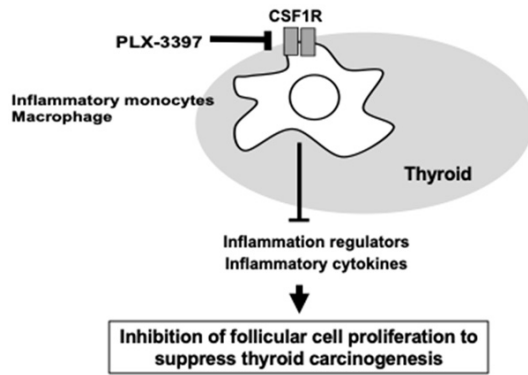
**Figure 7.** Schematic representation of a proposed model for the inhibition of follicular cell proliferation to suppress thyroid carcinogenesis of *Thrb$^{PV/PV}$Pten$^{+/-}$* mouse. PLX inhibits the CSF1R signaling, leading to the reduction of inflammatory monocytes and macrophages, and thus suppression of the expression and downstream signaling of inflammatory regulators and cytokines. These inhibitory changes lead to the inhibition of follicular cell proliferation and thereby suppression of thyroid carcinogenesis.

ronment-driven) and the intrinsic (oncogene-driven) [22]. The extrinsic pathways are triggered by the infiltrated leukocytes, tumor-associated macrophages, cytokines, and chemokines. The intrinsic pathways are mediated by the oncogenic alterations in the thyroid tumors. In the mouse model of follicular thyroid cancer (*Thrb$^{PV/PV}$Pten$^{+/-}$* mice) that was used in the present study, over-activated PI3K-AKT signaling is the primary event driving the carcinogenesis [13]. The findings that hyperplasia of follicular cells was accompanied by the infiltration of inflammatory monocytes prompted us to ponder what could be the initiator in these two pathways. It is known that in thyroid cancer, oncogenes promote proliferative effects on the tumor microenvironment (TME), influenced by transcriptional regulators such as NF-κB, PI3K-AKT, and MAPK [23]. In *Thrb$^{PV/PV}$Pten$^{+/-}$* mice, the major oncogenic event of PI3K-AKT signaling is driven by the oncogene, TRβPV, and PTEN-deficiency [13]. The downstream signaling of PI3K-AKT and networking events could lead to activation of transcription of genes that promote proliferation of TME. TME acts as a reservoir of pro-tumorigenic and pro-angiogenic cytokines, produced by tumor cells, and immune cells to further stimulate proliferation of tumor cells and recruitment of immune cells. Currently, it is not clear which pathway initiates and perpetuates the interrelated processes, resulting in eventual cancer

development. This question requires future studies.

The finding that hyperplasia of thyroid follicular cells was accompanied by infiltration of inflammatory monocytes and elevated immune-related regulators prompted us to test the hypothesis that attenuation of the inflammation would suppress hyperplasia. Accordingly, we treated *Thrb$^{PV/PV}$Pten$^{+/-}$* mice with PLX, an inhibitor of CSF1R. PLX was effective in impeding the infiltration of inflammatory monocytes and macrophages and in suppressing the expression of *Csf1r* and a panel of cytokines, and inflammation-regulatory genes. Remarkably, PLX potently inhibited the proliferation of thyroid follicular cells of *Thrb$^{PV/PV}$Pten$^{+/-}$* mice. These results demonstrated directly the critical stimulatory role of inflammation in promoting hyperplasia in the initial phase of thyroid carcinogenesis. Importantly, these findings clearly showed that suppression inflammation could prevent further progression of thyroid cancer. Thus, our studies have opened the possibility of a novel strategy for the prevention of thyroid cancer.

## Acknowledgements

## Disclosure of conflict of interest

None.

Address correspondence to: Dr. Sheue-Yann Cheng, Laboratory of Molecular Biology, Center for Cancer Research, National Cancer Institute, National Institutes of Health, 37 Convent Drive, Room 5128, Bethesda, Maryland 20892-4264, USA. Tel: 240-760-7828; Fax: 240-541-4498; E-mail: chengs@mail.nih.gov

## References

[1] Kaliszewski K. Does every classical type of well-differentiated thyroid cancer have excellent prognosis? A case series and literature review. Cancer Manag Res 2019; 11: 2441-2448.

[2] Baudino TA. Targeted cancer therapy: the next generation of cancer treatment. Curr Drug Discov Technol 2015; 12: 3-20.

[3] Landa I, Ibrahimpasic T, Boucai L, Sinha R, Knauf JA, Shah RH, Dogan S, Ricarte-Filho JC, Krishnamoorthy GP, Xu B, Schultz N, Berger MF, Sander C, Taylor BS, Ghossein R, Ganly I and Fagin JA. Genomic and transcriptomic hallmarks of poorly differentiated and anaplastic thyroid cancers. J Clin Invest 2016; 126: 1052-1066.

[4] Pozdeyev N, Gay LM, Sokol ES, Hartmaier R, Deaver KE, Davis S, French JD, Borre PV, LaBarbera DV, Tan AC, Schweppe RE, Fishbein L, Ross JS, Haugen BR and Bowles DW. Genetic analysis of 779 advanced differentiated and anaplastic thyroid cancers. Clin Cancer Res 2018; 24: 3059-3068.

[5] Bikas A, Vachhani S, Jensen K, Vasko V and Burman KD. Targeted therapies in thyroid cancer: an extensive review of the literature. Expert Rev Clin Pharmacol 2016; 9: 1299-1313.

[6] Widakowich C, de Castro G Jr, de Azambuja E, Dinh P and Awada A. Review: side effects of approved molecular targeted therapies in solid cancers. Oncologist 2007; 12: 1443-1455.

[7] Guarino V, Castellone MD, Avila E and Melillo RM. Thyroid cancer and inflammation. Mol Cell Endocrinol 2010; 321: 94-102.

[8] Melillo RM, Guarino V, Avila E, Galdiero MR, Liotti F, Prevete N, Rossi FW, Basolo F, Ugolini C, de Paulis A, Santoro M and Marone G. Mast cells have a protumorigenic role in human thyroid cancer. Oncogene 2010; 29: 6203-6215.

[9] Marcello MA, Cunha LL, Batista FA and Ward LS. Obesity and thyroid cancer. Endocr Relat Cancer 2014; 21: T255-271.

[10] Resende de Paiva C, Gronhoj C, Feldt-Rasmussen U and von Buchwald C. Association between Hashimoto's thyroiditis and thyroid cancer in 64,628 patients. Front Oncol 2017; 7: 53.

[11] Wang M, Zhao J, Zhang L, Wei F, Lian Y, Wu Y, Gong Z, Zhang S, Zhou J, Cao K, Li X, Xiong W, Li G, Zeng Z and Guo C. Role of tumor microenvironment in tumorigenesis. J Cancer 2017; 8: 761-773.

[12] Hanahan D and Weinberg RA. The hallmarks of cancer. Cell 2000; 100: 57-70.

[13] Guigon CJ, Zhao L, Willingham MC and Cheng SY. PTEN deficiency accelerates tumour progression in a mouse model of thyroid cancer. Oncogene 2009; 28: 509-517.

[14] Park JW, Han CR, Zhao L, Willingham MC and Cheng SY. Inhibition of STAT3 activity delays obesity-induced thyroid carcinogenesis in a mouse model. Endocr Relat Cancer 2016; 23: 53-63.

[15] Park S, Willingham MC, Qi J and Cheng SY. Metformin and JQ1 synergistically inhibit obesity-activated thyroid cancer. Endocr Relat Cancer 2018; 25: 865-877.

[16] Park S, Zhu J, Altan-Bonnet G and Cheng SY. Monocyte recruitment and activated inflammation are associated with thyroid carcinogenesis in a mouse model. Am J Cancer Res 2019; 9: 1439-1453.

[17] Stanley ER, Berg KL, Einstein DB, Lee PS, Pixley FJ, Wang Y and Yeung YG. Biology and action of colony--stimulating factor-1. Mol Reprod Dev 1997; 46: 4-10.

[18] Fixe P and Praloran V. Macrophage colony-stimulating-factor (M-CSF or CSF-1) and its receptor: structure-function relationships. Eur Cytokine Netw 1997; 8: 125-136.

[19] Merry TL, Brooks AES, Masson SW, Adams SE, Jaiswal JK, Jamieson SMF and Shepherd PR. The CSF1 receptor inhibitor pexidartinib (PLX3397) reduces tissue macrophage levels without affecting glucose homeostasis in mice. Int J Obes (Lond) 2020; 44: 245-253.

[20] Lin YH and Yang-Yen HF. The osteopontin-CD44 survival signal involves activation of the phosphatidylinositol 3-kinase/Akt signaling pathway. J Biol Chem 2001; 276: 46024-46030.

[21] Chung ES, Chauhan SK, Jin Y, Nakao S, Hafezi-Moghadam A, van Rooijen N, Zhang Q, Chen L and Dana R. Contribution of macrophages to angiogenesis induced by vascular endothelial growth factor receptor-3-specific ligands. Am J Pathol 2009; 175: 1984-1992.

[22] Mantovani A, Allavena P, Sica A and Balkwill F. Cancer-related inflammation. Nature 2008; 454: 436-444.

[23] Ferrari SM, Fallahi P, Galdiero MR, Ruffilli I, Elia G, Ragusa F, Paparo SR, Patrizio A, Mazzi V, Varricchi G, Marone G and Antonelli A. Immune and inflammatory cells in thyroid cancer microenvironment. Int J Mol Sci 2019; 20: 4413.

**Table S1.** Antibody list for FACS analysis

| Antibody | Clone ID | Purpose | Manufacturer |
|---|---|---|---|
| CD3e | 145-2C11 | Lineage Depletion | Tonbo |
| CD19 | 1D3 | Lineage Depletion | Tonbo |
| NKp46 (CD335) | 29A1.4 | Lineage Depletion | ebioscience |
| Ly6G (Gr-1) | 1A8 | Lineage Depletion | Tonbo |
| Sca-1 | D7 | Lineage Depletion | Biolegend |
| Ter119 | Ter119 | Lineage Depletion | Tonbo |
| Ly6C | HK1.4 | Sort | Biolegend |
| MHC-II | M5/114.15/2 | Sort | BD |
| cKit (CD117) | 2B8 | Sort | BD |
| CD115 | AFS98 | Sort | Biolegend |
| CD45 | 30-F11 | Sort | ebioscience |

**Table S2.** Primer list for RT-qPCR

| | Forward primer (5'-3') | Reverse primer (5'-3') |
|---|---|---|
| *Csf1* | TCATCGAGTGTGATGGGAAA | GGTGACTTGTTTCAGGCACA |
| *Csf1r* | CTTTTCGACGCTGCTTTCTC | CCATGGCACAGAACTTCCTT |
| *Spp1 (OPN)* | AGCAAGAAACTCTTCCAAGCA | GTGAGATTCGTCAGATTCATCCG |
| *Ptgs1* | GTGCTGGGGCAGTGCTGGAG | TGGGGCCTGAGTAGCCCGTG |
| *Aif1* | TGATGAGGATCTGCCGTCCAAACT | TCTCCAGCATTCGCTTCAAGGACA |
| *Sphk1* | GGCTCTGCAGCTCTTCCAGAG | CTCCTCTGCACACACCAGCTC |
| *Chil1* | AGAGGCCCTGACTAGGAAGC | GTGCACAGGAAAGGTTGGAT |
| *Il6* | CCTCTGGTCTTCTGGAGTACC | ACTCCTTCTGTGACTCCAGC |
| *Ccl9* | CAACAGAGACAAAAGAAGTCCACAC | CTTGCTGATAAAGATGATGCCC |
| *Ccl3* | ACCACTGCCCTTGCTGTTC | TCTGCCGGTTTCTCTTAGTCAG |
| *Ccl12* | AGAATCACAAGCAGCCAGTGT | ATCCAAGTGGTTTATGGAATTCTTAAC |
| *Ccr2* | GCCAGGACAGTTACCTTTGG | CGAAACAGGGTGTGGAGAAT |
| *Kit* | TCATCGAGTGTGATGGGAAA | GGTGACTTGTTTCAGGCACA |
| *Ephx2* | CTGGATACCCTGAAGGCAAA | TGACGTCATTTGGATTGCAT |
| *CD163* | CCTCCTCATTGTCTTCCTCCTGTG | ATCCGCCTTTGAATCCATCTCTTG |
| *Il15* | GTGACTTTCATCCCAGTTGC | TTCCTTGCAGCCAGATTCTG |
| *Ccl11* | GTCACTTCCTTCACCTCCCAG | ATCTCTTTGCCCAACCTGGT |
| *Cxcl13* | CAGGCCACGGTATTCTGGA | CAGGGGGCGTAACTTGAATC |

1